Covalent Attachment of Functional Proteins to Microfiber Surfaces via a General Strategy for Site-selective Tetrazine Ligation

Paramesh K. Ramaraj, Mugdha Pol, Samuel L. Scinto, Xinqiao Jia,* and Joseph M. Fox*

Authors

Paramesh K. Ramaraj, Department of Chemistry and Biochemistry, University of Delaware, Newark, DE 19716, USA

Mugdha Pol, Department of Biological Sciences, University of Delaware, Newark, DE 19716, USA

Samuel L. Scinto, Department of Chemistry and Biochemistry, University of Delaware, Newark, DE 19716, USA

Corresponding Authors

Xinqiao Jia, Department of Material Science and Engineering; Department of Biological Sciences, University of Delaware Newark, DE 19716, USA.

Joseph M. Fox, Department of Chemistry and Biochemistry; Department of Material Science and Engineering University of Delaware, University of Delaware Newark, DE 19716, USA.

Abstract

Surface modification of materials with proteins has various biological applications and hence the methodology for surface modification needs to accommodate a wide range of proteins that differ in structure, size, and function. Presented here is a methodology that uses the Affinity Bioorthogonal Chemistry (ABC) tag, 3-(2-pyridyl)-6-methyltetrazine (PyTz), for the site selective modification and purification of proteins and subsequent attachment of the protein to *trans*-cyclooctene (TCO) functionalized hydrogel microfibers. This method of surface modification is shown to maintain the functionality of the protein after conjugation with proteins of varying size and functionalities, namely HaloTag, NanoLuc luciferase (NanoLuc) and fibronectin type III domains 9-10 (FNIII 9-10). The method also supports surface modification with multiple proteins, which is shown with the simultaneous conjugation of HaloTag and NanoLuc on the microfiber surface. The ability to control the relative concentrations of multiple proteins presented on the surface is shown with the use of HaloTag and superfolder GFP (sfGFP). This application of ABC-tagging methodology expands on existing surface modification methods and provides flexibility in the site-selective protein conjugation methods used along with the rapid kinetics of tetrazine ligation.

Keywords

Biomaterials, Site-selective, Protein, Tetrazine, trans-Cyclooctene, Gradient, Scaffold, 3D Cell Culture

Introduction

Surface modification of materials with proteins is used in many applications, such as the fabrication of biosensors,[1, 2] preparation of substrates for cell culture[3, 4] and modifications of materials for biological applications.[5, 6] Across this range of applications, the proteins used also vary in size, functionality, and stability. Hence, the methodology used to functionalize materials needs to accommodate a wide range of proteins, with the retention of protein functionality after modification being paramount. While biomaterials can be functionalized by adsorption of the protein, this approach does not offer control over protein orientation with respect to the surface, and is frequently associated with protein denaturation, leading to reduction or loss of protein function.[2, 7] Additionally, physical adsorption does not offer control over initial protein loading and suffers from desorption.[8, 9] The use of covalent chemistry to modify a material's surface offers a distinct advantage in terms of controlling protein loading and providing a sustained presence. Site-specific modification of the protein for covalent attachment enables control over protein orientation and the maintenance of the secondary and tertiary structures. Site-selective attachment of proteins to material interfaces is necessary to mimic signaling complexes found in cell-cell and cell-extracellular matrix interfaces.[10] Site specific labeling as opposed to residue wide labelling, such as lysine modification, also ensures that functional resides of proteins such as those in enzymatic active sites or binding pockets are not adversely affected.[11, 12] Site specific modification also ensures homogeneity of the modified protein which ensures even bioactivity of the protein across the entire biomaterial.[13] Cysteine residues, which can be introduced via genetic encoding, can sometimes be used for site-selective protein modification.[14] However, this approach is generally limited to proteins that have only one reactive cysteine. Additionally, cysteine modifications of proteins proceed with varying levels of competing disulfide formation, giving a mixture of alkylated and non-alkylated proteins which may be inseparable. Furthermore, for many proteins, cysteines can be essential to protein activity and their modification in those situations is not a viable strategy.

Materials can be covalently modified with a range of different bioorthogonal reactions[2, 13, 15] including oxime ligation[16, 17], Staudinger ligation[18, 19], CuAAC[20-23], and SPAAC[24, 25] reactions. The relatively slow kinetics of most bioorthogonal reactions can present a limitation to surface modification with biological molecules, as the required high concentration of labeling reagent can be impractical for biomolecular samples due to cost, solubility and concerns about non-specific binding. It has been shown that faster bioorthogonal reactions can lower the concentration requirements for protein conjugation while also providing better retention of protein activity. [26] The bioorthogonal tetrazine ligation, the inverse electron demand Diels-Alder reaction between *s*-tetrazine (Tz) and *trans*-cyclooctene (TCO), was described in 2008 by our group.[27] The very fast bimolecular rate constants for tetrazine ligations range from k_2 10^4 – 10^6 M^{-1} s^{-1},[28] making this reaction well suited for the for biomaterials applications[29, 30] including functionalization of surfaces with biological molecules. The use of tetrazine-TCO ligation for protein immobilization on glass slides was first described in 2013.[31, 32] In 2016, our groups showed that tetrazine-TCO ligation could be used for site-selective conjugation of fluorescent proteins to the surface of tetrazine-functionalized hydrogel microfibers.[33] Mehl has shown that the use of tetrazine chemistry improves the retention of structure and activity in immobilized proteins.[26, 34] Surfaces of glass, titanium, silicon, hydrogels and thermoplastic elastomers have been functionalized with a number of proteins via tetrazine ligation.[26, 32, 34-40] Antibodies were covalently immobilized on the surface of microplates by tetrazine ligation to improve the sensitivity of ELISA assay.[41] However, in a

majority of these applications, the conjugation of Tz or TCO to the proteins of interest was not performed site-specifically.

Biomaterials that can mimic the structure and function of fibrous components of the 3-dimensional extracellular matrix can serve as scaffolds for guiding cellular behavior and migration as well as the reconstruction of damaged tissue.[42] Previous work in our lab has made use of tetrazine ligation in the synthesis of cytocompatible hydrogel microfibers.[33, 43-45] With rapid kinetics, this reaction enabled the construction of meter-long polymer microfibers via interfacial polymerization. In this experiment, a hydrophobic bis- or tris-TCO monomer dissolved in ethyl acetate was layered on top of an aqueous solution containing a poly(ethylene glycol) (PEG)-based bis-tetrazine monomer. Upon contact at the solvent-water interface, a polymer film formed instantaneously, which was continuously pulled out of the interface to produce microfibers. Cell-adhesive microfibers were prepared using a PEG-based bis-Tz monomer with dangling RGD (arginine-glycine-aspartic acid) peptide.[43] While high concentrations of the RGD peptides promote cell adhesion to the hydrogel fibers, the simplified peptide motif does not represent the full function of the intact proteins or the domains from which they are derived.

To assay whether full-length proteins retain functionality after incorporation into the microfibers, we previously adapted this interfacial polymerization approach to the synthesis of green fluorescent protein (GFP)-modified microfibers, either by introducing a superfolder GFP-tetrazine (sfGFP-Tz) during the interfacial polymerization using a genetically encoded tetrazine,[44] or by post-polymerization modification of tetrazine-containing microfibers with TCO-functionalized Clover, a variant of GFP.[33] However, the high stability of GFP[46, 47] can make it a poor model for many proteins that are much more prone to denaturation/loss of function. In these studies, GFP was modified either via cysteine-maleimide conjugation or via genetic code expansion using tetrazine-based unnatural amino acid pioneered by Mehl.[48, 49]

In addition to our work in functionalizing microfibers with sfGFP with a genetically encoded tetrazine,[44] surfaces of silicon wafers have been functionalized with carbonic anhydrase with a genetically encoded tetrazine for controlled load and orientation.[26, 34] Genetic code expansion provides both site selectivity and homogeneity, however, it requires additional plasmids and protein yields vary depending on the suppression site on the protein as well as the nature of the protein itself.[34, 50] We therefore sought to develop a method for protein functionalization that was general, site-selective, and retained protein activity after surface immobilization.

Recently, our group developed a general platform for site-selective functionalization of proteins with 3-(2-pyridyl)tetrazines, which can not only participate in rapid biorthogonal chemistry but also facilitate protein purification as affinity tags capable of binding to Ni-IDA resins commonly used with His-tagged proteins. These Affinity Bioorthogonal Chemistry (ABC) tags work with a range of site-selective bioconjugation methods with proteins tagged at the C-terminus, N-terminus or internal positions.[51] Since the site-selectively attached tetrazine also functions as the purification tag, this results in the synthesis of pure homogenous modified proteins without the need for extensive purification steps or genetic code expansion. Herein, we demonstrate that ABC-tagging in tandem with tetrazine ligation to conjugate site-selectively functionalized proteins to TCO-modified hydrogel microfiber surfaces (Figure 1). This methodology allows for the site-selective covalent attachment of tetrazine modified proteins on TCO-modified material surfaces with ultra-fast chemistry. The microfibers serve as a well-defined synthetic biocompatible material surface

to demonstrate the site-selective attachment of active proteins. The hydrogel microfibers also enable the use of fluorescence microscopy and plate reader luminescence assays for the convenient readout of protein activity after conjugation. In addition, the cytocompatibility of the

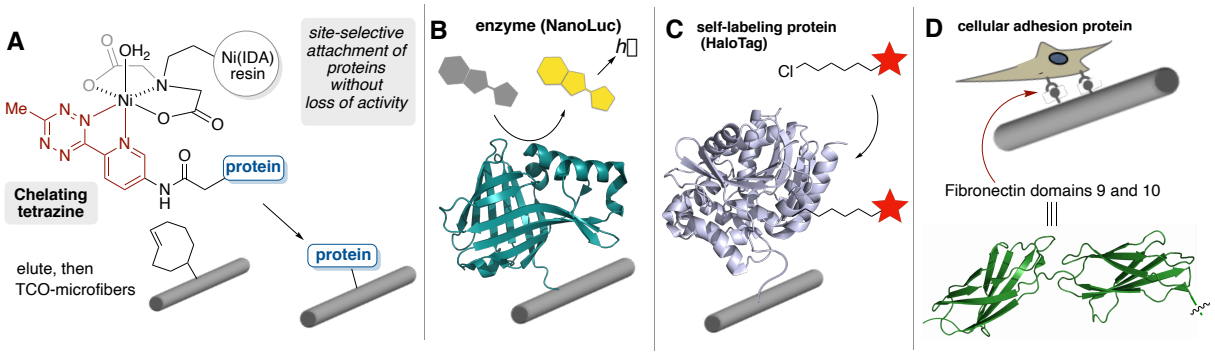

Figure 1. (A) Workflow for functionalization of microfibers with native proteins. Single-tagged proteins were prepared either by C-terminal sortase ligation or via cysteine-alkylation, conjugated to a chelating tetrazine (ABC-Tag), purified by Ni resin chromatography and subsequently conjugated to TCO functionalized microfibers. (B-D) The different proteins that were used to functionalize the microfibers. NanoLuc luciferase (NanoLuc) catalyzes the conversion of furimazine to furimamide with the emission of light. HaloTag is a self-labeling enzyme that covalently attaches a ligand that is connected to a chloroalkane linker to its active site. Domains 9 and 10 of fibronectin (FNIII 9-10) help to attach cells on to the surface of the microfibers and allow the cells to proliferate on the fibers.

hydrogel microfibers permits evaluation of the function of immobilized ECM protein to promote cell adhesion and proliferation. The microfibers can be manipulated to fit into standard well plates, on microscope slides and as scaffolds which makes them a suitable substrate for these applications. We show that proteins conjugated to the microfibers via late-stage functionalization maintained their function, whereas introducing the protein during interfacial polymerization led to a loss of function. We show that HaloTag protein conjugated to the microfibers was capable of self-labeling reactions, and the immobilized NanoLuc luciferase (NanoLuc) enzyme can produce bioluminescence. Importantly, microfibers with dually functionalized HaloTag and Nanoluc retained the activity of both proteins. We also functionalized the fibers with HaloTag and sfGFP and showed that we can control the relative concentrations of proteins on the microfibers. Finally, we show that conjugation of fibronectin type III domains 9-10 (FNIII 9-10) gave rise to microfibers that fostered the attachment and proliferation of fibroblast cells and kidney epithelial cells.

Materials and Methods

Fiber Pulling. Interfacial polymerization was performed according to the previously published procedure.[33] Briefly, bis-Tz (**2**) was dissolved in water at a concentration of 1 mg/mL and bis-TCO-DHTz (**1**) was dissolved in ethyl acetate at a concentration of 1 mg/mL. The bis-Tz (**2**) solution was added to a 60 mm diameter petridish (3 mL of solution) or a 20 mL scintillation vial (1 mL of solution) with the top cut off. An equal volume of bis-TCO-DHTz (**1**) solution was layered on top carefully. Upon contact a thin polymer film forms at the interface. The thin film was grasped firmly with a sharp pair of tweezers and the fiber was pulled from the interface and collected on to a copper wire frame. The fibers were affixed onto glass slides or into 24 well plates using adhesive silicone isolators. Fibers synthesized with the tris-TCO (**4, Figure S3**) crosslinker was

made the same way, with the tris-TCO monomer in the organic layer instead of bis-TCO-DHTz (**1**).

Late-stage Labeling of Fibers with HaloTag. Fibers were made form bis-TCO-DHTz (**1**) and bis-Tz (**2**) as described above and affixed on glass slides with silicone isolators. The fibers were first soaked in a solution of PBS containing sTCO-acid (**5, Figure S3**) (1 mM, 100 μL) for two minutes to cap off any unreacted tetrazine end groups from the monomer. The fibers were then washed with PBS containing 0.25% Tween 80 (PBST) by immersing the fibers in the buffer for five minutes, and then replacing the buffer with fresh PBST. This process was repeated three times. The fibers were then soaked in solution of methylene blue in water (100 μM, 100 μL) and irradiated with a red LED light (λ_{max} = 658 nm, 150 mW/cm^2) for 5 minutes. The fibers were then washed with PBST (3×5 min). The fibers were then soaked in a solution of the bis-TCO linker (**3**) in water (1 mM, 100 μL) for 5 minutes. The fibers were then washed with PBST (3×5 min). The fibers were labeled with a solution of HaloTag-Tz in PBS (2.5 μM, 100 μL) for 30 minutes. The fibers were then washed with PBST (3×5 min). The HaloTag protein on the fibers was then labeled with a solution TAMRA-Cl (**6, Figure S3**) in PBS (2 μM, 100 μL) for 30 minutes. The fibers were then washed with PBST (3×5 min) and allowed to soak in PBST overnight at room temperature, protected from light. The fibers were washed with PBS (150 μL, 3×5 min) before imaging. Protein labeling on fibers without methylene blue was also performed the same way as described above, except the fibers were soaked in PBS during irradiation. The fibers were imaged on an EVOS FL Auto 2 in order to obtain the fluorescence and brightfield images. The fluorescence intensity of each fiber was measured using ImageJ with the 'Mean Gray' function. This was background corrected by subtracting the intensity of the fluorescence in the area around the fibers. The area of the fibers was calculated from the length and width of the fibers measured using ImageJ. The background corrected fluorescence intensity of each fiber was divided by the area of the fiber to obtain the final fluorescence intensity. This analysis was carried out for all fibers in the image and the mean fluorescence of the fibers in the image was calculated. The process was repeated for three slides each for the photoactivated and non-photoactivated fibers, and the mean fluorescence intensity of the fibers for the photoactivated and non-photoactivated condition was then calculated. For statistical analysis, *t* tests were performed using an online calculator (https://www.graphpad.com/quickcalcs/ttest1/).

Labeling of Fibers with NanoLuc. Bis-TCO-DHTz fibers (synthesized from **1** and **2**) affixed into 24 well plates were photoactivated and functionalized with bis-TCO linker (**3**) and labeled with Nanoluc-Tz (2.5 μM in 100 μL PBS) the same way as described for HaloTag. After overnight soaking in PBST, the fibers were washed PBS (150 μL, 3×5 min). Furimazine (**7, Figure S3**) (10 μM in 100 μL PBS) was added to the fibers and the luminescence reading was immediately measured using a Tecan Spark plate reader. The length and width of the individual fibers were also measured using an EVOS FL Auto 2 microscope by obtaining a brightfield image of the entire well. ImageJ was used to calculate the area for all fibers in the well, which was used to calculate the mean area of the fibers. The luminescence readings obtained were divided by the mean area of the fibers to obtain the final luminescence value. This analysis was carried out with three wells each for the photoactivated and non-photoactivated fibers, and the mean luminescence reading for each condition was then calculated. For statistical analyses, *t* tests were performed using an online calculator (https://www.graphpad.com/quickcalcs/ttest1/).

Sequential Labeling of Fibers with NanoLuc followed by Halotag. Bis-TCO-DHTz fibers (synthesized from **1** and **2**) affixed into 24 well plates were photoactivated and functionalized with bis-TCO linker (**3**) and labeled with Nanoluc-Tz (1.25 μM in 100 μL PBS) for 30 minutes as

described above. The fibers were then washed with PBST (3×5 min). The fibers were then incubated with HaloTag-Tz (1.25 μM in 100 μL PBS) for 30 minutes. The fibers were then washed with PBST (3×5 min). The HaloTag protein on the fibers was then labeled with a solution TAMRA-Cl in PBS (2 μM, 100 μL) for 30 minutes. The fibers were then washed with PBST (3×5 min) and allowed to soak in PBST overnight at room temperature, protected from light. The fibers were washed with PBS (150 μL, 3×5 min) and subsequently imaged and then used for luminescence measurements following addition of furimazine.

Sequential Labeling of Fibers with Halotag followed by NanoLuc. Bis-TCO-DHTz fibers (synthesized from **1** and **2**) affixed into 24 well plates were photoactivated and functionalized with bis-TCO linker (**3**) and labeled with HaloTag-Tz (1.25 μM in 100 μL PBS) for 30 minutes as described above. The fibers were then washed with PBST (3×5 min). The fibers were then incubated with Nanoluc-Tz (1.25 μM in 100 μL PBS) for 30 minutes. The fibers were then washed with PBST (3×5 min). The HaloTag protein on the fibers was then labeled with a solution TAMRA-Cl in PBS (2 μM, 100 μL) for 30 minutes. The fibers were then washed with PBST (3×5 min) and allowed to soak in PBST overnight at room temperature, protected from light. The fibers were washed with PBS (150 μL, 3×5 min) and subsequently imaged and then used for luminescence measurements following addition of furimazine.

Simultaneous Labeling of Fibers with NanoLuc and Halotag. Bis-TCO-DHTz fibers (synthesized from **1** and **2**) affixed into 24 well plates were photoactivated and functionalized with bis-TCO linker (**3**). Simultaneous labeling of the fibers with NanoLuc-Tz and HaloTag-Tz was carried out by mixing the proteins together at an equimolar concentration of 1.25 μM in 100 μL PBS and incubating the fibers with the protein mixture for 30 minutes. Subsequent washing, imaging and luminescence measurements were carried out as described above.

Labeling of Fibers with HaloTag and sfGFP. Bis-TCO-DHTz fibers (synthesized from **1** and **2**) affixed on glass slides were photoactivated and functionalized with bis-TCO linker (**3**) as described before. The fibers were co-incubated with a solution of HaloTag-Tz (500 nM) and sfGFP-Tz (varied from 100 nM – 500 nM) in 100 μL phosphate buffer for 30 minutes. The fibers were then washed with PBST (100 μL, 3×5 min). The fibers were then incubated with a solution of TAMRA-Cl (2 μM in 100 μL PBS) for 30 minutes. The fibers were washed with PBST (100 μL, 3×5 min) and then allowed to soak in PBST (200 μL) overnight at room temperature, protected from light. The next day, the fibers were washed with PBS (100 μL, 3×5 min) and imaged on an EVOS M7000 for the fluorescence output of HaloTag-TAMRA and sfGFP. The fluorescence intensity of each fiber was measured using ImageJ with the 'Mean Gray' function. This was background corrected by subtracting the intensity of the fluorescence in the area around the fibers. The area of the fibers was measured from the length and width of the fibers using ImageJ. The background corrected fluorescence intensity of each fiber was divided by the area of the fiber to obtain the final fluorescence intensity. This analysis was carried out for all fibers in an image and was used to calculate the mean fluorescence intensity of the fibers in the image. This experiment was repeated two more times for a total of three trials. Then the mean fluorescence intensity of the fibers for each condition was calculated.

Labeling fibers with FNIII 9-10. pHEMA solution (Poly (2-hydroxyethyl methacrylate)) (Santa Cruz Biotechnologies, Dallas, TX) was prepared at 20 mg/ml and coated on surface of 35 mm glass-bottomed Petri dish l No. 1.5 coverslip and allowed to cure at 37°C for 12 h to create non-adhesive cell culture surface. Fibers were pulled on to a 2 cm X 2 cm square steel wire frame and sprayed with 70% ethanol before being placed on to a pHEMA coated petri dish, inside a biosafety

cabinet. The fibers were irradiated with UV light for 20 minutes before the labeling protocol. The bis-TCO-DHTz fibers (synthesized from **1** and **2**) were photoactivated, functionalized with bis-TCO linker (**3**) and labeled with 5 μM of FNIII 9-10-Tz according to the protocol specified above, with the use of DPBS for all washing steps instead of PBST. The tris-TCO fibers (synthesized from **4** and **2**) contained 5 μM of FNIII 9-10-Tz in the aqueous layer prior to being pulled on to a 2 cm X 2 cm square steel wire. They were sterilized the same way as the bis-TCO fibers. All fibers were incubated in DPBS overnight in the fridge before cell seeding the next day. The scaffold was washed with 1X PBS 3 times and equilibrated with serum free basal cell culture media for 2 h, before start of cell culture.

Cell culture of MDCK and NIH 3T3 fibroblasts. MDCK cells and NIH 3T3-GFP cells were purchased from the American Type Culture Collection (ATCC, Manassas, VA) and Cell Biolabs (San Diego, CA) respectively. NIH 3T3 cells were maintained in Dulbecco's Modified Eagle Medium (DMEM) with 10% (v/v) fetal bovine serum (HyClone FBS) and 1% (v/v) penicillin-streptomycin, while MDCK cells were maintained in Eagle's Minimum Essential Medium (EMEM) with 10% (v/v) fetal bovine serum (Hyclone FBS) and 1% (v/v) penicillin-streptomycin at 37°C with 85% humidity and 5% CO_2. Media was refreshed every 2 days. After reaching 80% confluency, the cells were passaged using 0.25% (w/v) trypsin containing ethylenediaminetetraacetic acid (2.2 mM, EDTA-4Na). Experiments were conducted with at least three different passages between 10-20 for each cell type. Cells were seeded at $0.5x10^6$ cells/ml for MDCK cells and $1x10^6$ cells/ml for NIH3T3 fibroblasts on top of the fiber scaffold and incubated for 5 days in respective cell culture media.

Live/Dead Assay: After 1, 3 and 5 days of culture, MDCK cells were incubated with Calcein AM (Thermo Fisher Scientific, cat. no: C1430), ethidium homodimer (Thermo Fisher Scientific, cat. no: E1169) and Hoechst 33342 (Life Technologies, cat. no: H3570) at a final concentration of 4 µM, 2 µM and 6 µM respectively in warm PBS at 37°C for 15 min. The dye solution was aspirated gently after 15 min and washed twice with 1X PBS. The samples were imaged using Zeiss LSM 880 confocal microscope (Carl Zeiss, Oberkochen, Germany). Images were acquired using Fluar 5X/0.25 air objective from at least three biological repeats for all fiber types at each time point. Images were captured with 10 µm z-axis step size, each 12-bit, and processed as maximum intensity projections using Zen 3.0 SR software.

Immunofluorescence: Cell-populated fiber scaffolds were washed with 1x PBS three times and fixed with 4% (w/v) paraformaldehyde (PFA, Sigma Aldrich) in PBS for 15 min. Samples were permeabilized in 0.2% (v/v) Triton X-100 in PBS for 2 h at room temperature. Blocking was done in 3% (w/v) bovine serum albumin in PBS for 2 h at room temperature. Primary antibody for Ki-67 (Abcam, cat. no: ab15580) was diluted in 3% BSA at 1:50 dilution and incubated overnight at 4°C. The primary antibody solution was aspirated gently, and samples were washed twice using PBS with 0.05% Tween 20 (PBST). Secondary antibody Alexa Fluor™ 488 goat anti-rabbit, along with Alexa Fluor™ 568 phalloidin (Life Technologies, Carlsbad, CA), diluted at 1:500 in 3% BSA, were added in samples and incubated for 2h at room temperature. The solution was aspirated and washed with PBST three times. Nuclei were counter-stained with DAPI (DAPI, Life Technologies, Carlsbad, CA), diluted at 1:1000 in PBS, for 15 min at room temperature. After washing three times with PBST, samples were stored at 4°C. Confocal microscopy was conducted using Zeiss LSM 880 with Fast Airyscan mode with 10X/0.45W Plan Apochromat water objective. Images were captured with 1.0 µm z-axis step size, each 16-bit. The brightness was evenly adjusted for

each channel and images were processed as maximum intensity projections using Zen 3.0 SR software.

Results and Discussion

Tetrazine-functionalized Proteins and TCO-based Monomers

ABC tagging was leveraged for the synthesis of tetrazine functionalized proteins. As FNIII 9-10 lacks any cysteine residues, we prepared a mutant with a genetically encoded cysteine at the N-terminal followed by modification by cysteine alkylation. Using the ABC-tagging approach, 3-(2-pyridyl)-6-methyltetrazine (PyTz) was conjugated to FNIII 9-10 at the N-terminus by cysteine alkylation followed by purification by Ni-NTA resin to provide pure protein conjugate (Figure 2A, Figure S15). For HaloTag and NanoLuc proteins, introducing a cysteine mutation was not a viable approach as HaloTag and NanoLuc already contain cysteine, prohibiting site-selective alkylation. Sortase-mediated ligation has been used for the generation of proteins such as enhanced green fluorescent protein, mCherry, mCerulean, β-lactamase and epidermal growth factor with biorthogonal handles for the functionalization of hydrogels.[52, 53] As shown in Fig 2B, HaloTag and NanoLuc were expressed with a sortase tag (LPETGG) at the C-terminus of the protein, through which PyTz was conjugated via sortase (SrtA7M) enzyme mediated ligation.[51, 54] Sortase-mediated ligation provided a convenient method to modify HaloTag (Figure S2A-B) and NanoLuc (Figure S2C-D). While sortase ligation produces a mixture, the PyTz-tagged proteins were readily purified by Ni resin chromatography. Compounds **1**, **2** and **3** (Figure 2C) were used to prepare TCO-functionalized microfibers. The hydrophobic bis-TCO monomer **1** contains a dangling, latent dihydrotetrazine (DHTz) moiety that can be photocatalytically activated to tetrazine after the microfiber is pulled out of the solvent-water interface. The PEG-based bis-tetrazine (bis-Tz) monomer **2** is water soluble and is necessary for microfiber synthesis (Figure 2B). Both **1** and **2** were made as previously described.[33] The PEG-based bis-TCO linker (**3**, Figure 2B), synthesized as described in the Supporting Information (Figure S1), is introduced for fiber modification post-polymerization to decorate microfibers with TCO groups through reaction with tetrazine, generated from DHTz after photocatalysis.

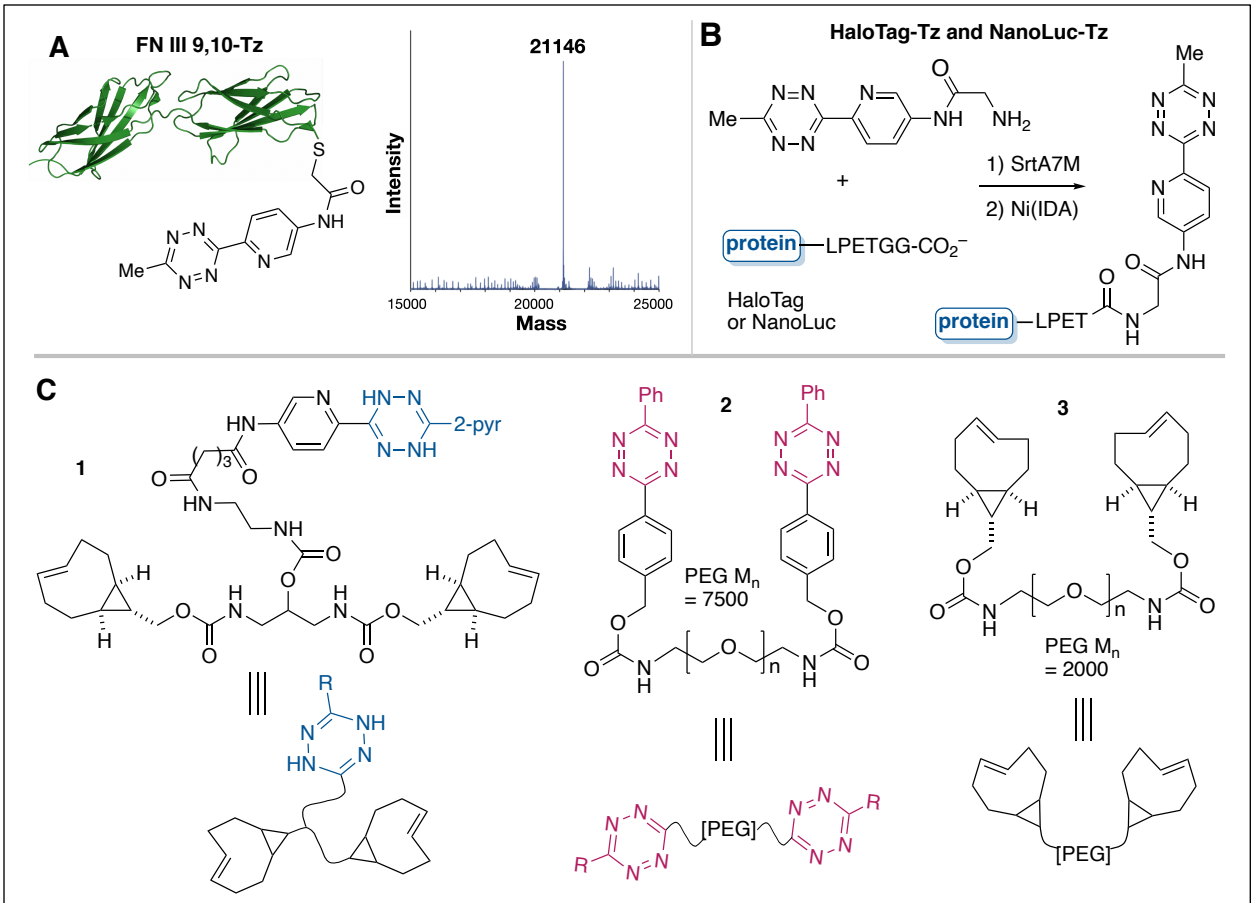

Figure 2. (A) FNIII 9-10 was functionalized with ABC-Tag by cysteine ligation and purified by Immobilized Metal Affinity Chromatography (IMAC) with Ni-IDA resin using the tetrazine as the affinity ligand. (B) NanoLuc and HaloTag were prepared as previously described via C-terminal ABC-Tag attachment via Sortase ligation and purified by IMAC using the tetrazine as the affinity ligand. (C) Compounds **1** and **2** were used as monomers for the synthesis of the microfibers via interfacial polymerization. **3** was used to functionalize the microfibers with TCO after photocatalytic activation of DHTz to Tz, for subsequent attachment of ABC tagged proteins.

Protein Immobilization during Microfiber Synthesis Leads to Loss of Activity

Initially, we attempted to incorporate proteins into microfibers during interfacial polymerization. This method was previously applied to sfGFP, which maintained fluorescence after the microfiber was produced.[44] However, sfGFP is not representative of most proteins because it is highly resilient toward denaturation.[47] HaloTag protein was therefore chosen for further study. HaloTag is a modified bacterial dehalogenase of 35 kDa capable of forming covalent conjugates through self-labeling of chloroalkane ligands to its active site.[55] When **HaloTag-Tz** (Figure 2B) was directly added to the aqueous phase containing PEG-bisTz, and microfibers were pulled out of the interface, passing through an organic phase of ethyl acetate containing a tris-TCO monomer (Figure S6A), the protein lost its activity. TAMRA-chloroalkane (TAMRA-Cl) (Figure S3) was

added to the microfibers as the substrate for conjugated HaloTag and functioned as a fluorescent reporter to assay the protein activity. The microfibers were imaged by fluorescence microscopy and were found to be only weakly fluorescent, indicating that the protein had possibly denatured during the fiber-pulling process (Figure S6C). This was in stark contrast to the control experiment where HaloTag-Tz was pre-reacted with TAMRA-Cl (Figure S4) before being added to the aqueous layer. Fibers thus synthesized were five times as fluorescent (Figure S6D) as compared to those prepared above with TAMRA-Cl added after fiber pulling. Under this condition, denaturation of HaloTag did not affect TAMRA fluorescence since it was conjugated prior to interfacial polymerization. These experiments with HaloTag protein showed that the direct inclusion of tetrazine-derived proteins during interfacial polymerization significantly compromised protein function, presumably due to protein denaturation when exposed to the organic solvent during the fiber-pulling process. As discussed in detail below, application of this procedure to FNIII 9-10 also led to loss of activity. Therefore, we sought an alternative method for functionalizing the fibers with a wider range of proteins.

Late-stage, Site-selective Conjugation Gives Fibers Bearing Functional Proteins

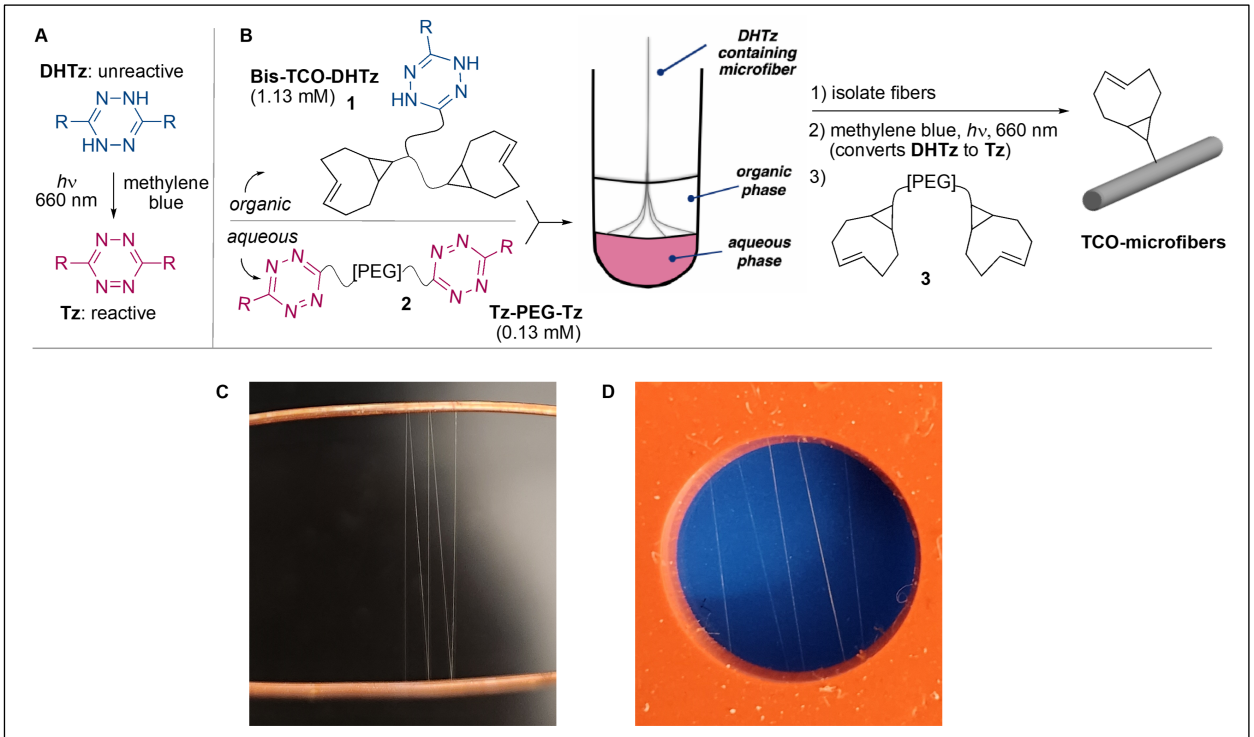

Figure 3. Synthesis of TCO-microfibers. (A) Inactive Dihydrotetrazine (DHTz) can be converted to tetrazine with the use of photocatalyst and light. (B) Schematic for the functionalization of DHTz fibers with TCO sites. (C-D) Microfibers were pulled from a glass dish on to a copper wire frame and affixed on to glass slides using a silicone isolator. DHTz was oxidized to Tz by the addition a solution of methylene blue (100 μM) followed by irradiation with red light for five minutes. A solution of bis-TCO (1 mM) was added to the fibers to functionalize the surface with TCO sites for subsequent protein attachment.

This approach started with preparation of microfibers containing dihydrotetrazine (DHTz) groups.[33] DHTz groups are unreactive towards TCO but, upon photocatalyzed oxidation, convert

to tetrazines, which engage in bioorthogonal chemistry (Figure 3A). Following our reported strategy, we prepared microfibers containing latent DHTz groups. Robust microfibers were pulled from the liquid-liquid interface (Figure 3B) and collected on a copper frame (Figure 3C). Fibers synthesized via interfacial tetrazine ligation are approximately 10 microns in diameter when dry, and approximately 25 microns in diameter when hydrated.[43, 44] The DHTz fibers were transferred onto a glass slide and secured in a silicone well (Figure 3D), and the latent DHTz groups were photocatalytically oxidized to tetrazines using methylene blue and red LED light. Exposure of tetrazine functionalized microfibers to an aqueous solution of 1 mM bis-TCO **3** (Figure 2C) for five minutes led to the conversion of surface tetrazine groups to the corresponding TCO moieties, providing a bioorthogonal handle to which Tz-functionalized proteins can be immobilized.

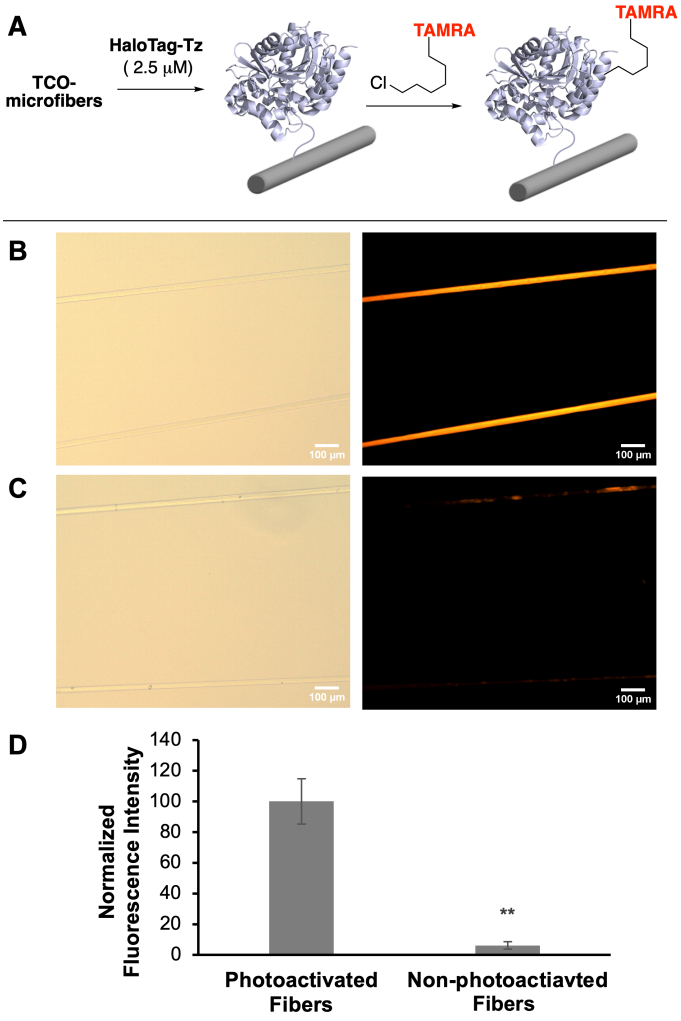

Figure 4. (A) A solution of HaloTag-Tz (2.5 μM) was added to the fibers and incubated for 30 minutes. Then, a solution of TAMRA-Cl (2 μM) was added to the fibers and incubated for 30 minutes to fluorescently label HaloTag. (B,C) Brightfield (left) and fluorescent (right) microscopy images of (B) photoactivated and (C) non-photoactivated fibers. (D) Quantification of HaloTag conjugation was carried out by densitometry analysis across an area containing two fibers. For each image, fluorescence was normalized to total fiber area as measured in the brightfield channel (n = 3, **: $p < 0.01$). The photoactivated fibers were, on average, sixteen times as fluorescent as the non-photoactivated fibers controls.

We used HaloTag to assay the activity of the protein after late-stage functionalization of the microfibers (Figure 4A). **HaloTag-Tz** (2.5 μM) was conjugated to the TCO-functionalized microfibers. Analysis by fluorescence microscopy (Figure 4B, Figure S7A) shows that the fibers are fluorescent after the addition of TAMRA-Cl, indicating that HaloTag was successfully attached to the fibers and the protein remained active after immobilization. Control fibers were not photoactivated and should not have any TCO sites for protein attachment. This is confirmed by fluorescence microscopy (Figure 4C, Figure S7B), which shows weakly fluorescent microfibers. Using ImageJ, the fluorescence intensity was measured. Our results show that the fluorescence signal of the photoactivated fibers is sixteen times as intense as the non-photoactivated fibers. The weak

fluorescence in the control fibers may be due to minor background oxidation of DHTz in the absence of photocatalyst and the generation of a small amount of TCO sites after post-polymerization modification with bis-TCO.

Given the positive result with HaloTag, we wanted to assay whether the late-stage functionalization method could serve as a general platform for protein attachment. We chose NanoLuc luciferase (NanoLuc) as a second protein to test the method. NanoLuc is a 19 kDa enzyme that catalyzes the conversion of the substrate furimazine (Figure S3) to furimamide with the emission of light and is commonly used for bioluminescent assays.[56] Therefore, NanoLuc is distinct from HaloTag in both size and functionality. **NanoLuc-Tz** (Figure 2B) was made using the same method as HaloTag-Tz.

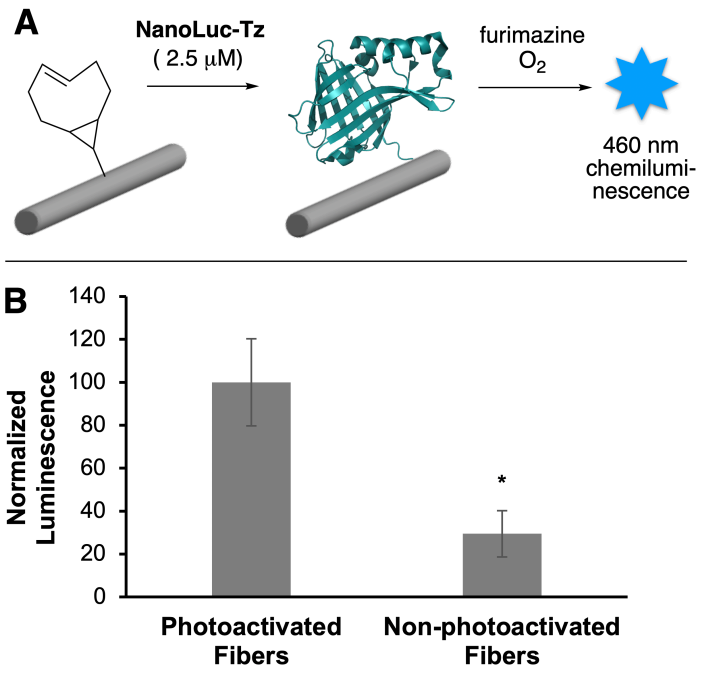

Figure 5. (A) A solution of NanoLuc-Tz (2.5 μM) was added to the fibers and incubated for 30 minutes. The fibers were washed overnight to removed unbound protein. A solution of furimazine (100 μM) in PBS was added to the fibers and the luminescence was measured using a plate reader. (B) Luminescence results of the photoactivated and non-photoactivated fibers. For each image, luminescence was normalized to total fiber area as measured in the brightfield channel in a microscopy image of the entire well (Figure S8) (n = 3, *: $p < 0.05$). The photoactivated fibers were, on average, five times as luminescent as the non-photoactivated fibers controls.

NanoLuc-Tz (2.5 μM) was introduced to the well containing affixed microfibers (Figure S5). Next, an aqueous solution of furimazine (100 μM) was added to the fibers (Figure 5A), and the luminescence was measured using a plate reader. The photoactivated fibers display a luminescence value five times that of the non-photoactivated control fibers (Figure 5B). The luminescence from control fibers was possibly due to background oxidation of DHTz or non-specific absorption of the protein onto the plastic surface of the well plate in which the fibers were embedded.

Late-stage Functionalization of Microfibers Supports Multiple Functional Proteins

To demonstrate that the microfibers could support multiple proteins, we functionalized the fibers with both HaloTag and NanoLuc. Mehl and coworkers have elegantly demonstrated that tetrazine ligation can be used for protein-limited conjugation to TCO-functionalized surfaces including SAMs and beads.[34] Protein-limited conjugation could theoretically be used here for the sequential addition of proteins to TCO-microfibers provided that the total number of TCO sites on the fiber substrate was sufficiently high and could be reliably measured. However, this approach is

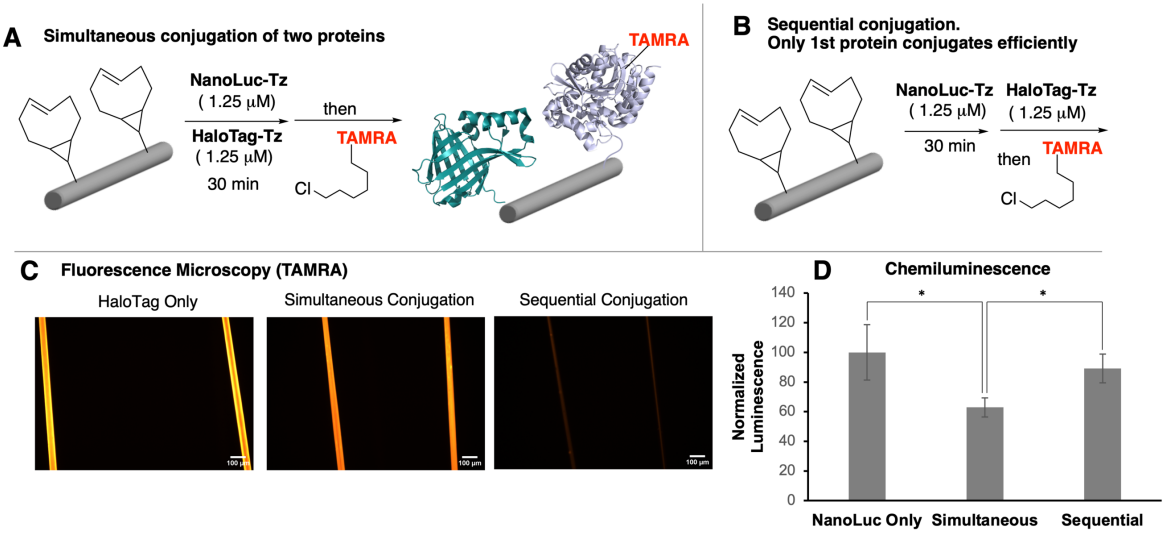

Figure 6. (A) For simultaneous conjugation, the microfibers were incubated with a solution of both NanoLuc-Tz and HaloTag-Tz at an equimolar concentration (1.25 μM) for 30 minutes. TAMRA-Cl and furimazine were subsequently added to obtain fluorescence and luminescence readouts. (B) For sequential conjugation, the fibers were incubated with a solution of NanoLuc-Tz (1.25 μM) first and then HaloTag-Tz (1.25 μM). TAMRA-Cl and furimazine were subsequently added to get fluorescence and luminescence readouts. (C) Fluorescence microscopy images obtained displaying the difference in fluorescence intensity of simultaneous conjugation and sequential conjugation in comparison to microfibers conjugated to only HaloTag (D) Luminescence readout obtained for simultaneous conjugation and sequential conjugation in comparison to microfibers conjugated to only NanoLuc. (n = 3, *: $p < 0.05$).

challenged by the small sample size and variations in total fiber loading and thickness, and hence, total number of TCO-sites per sample. As an alternate approach, we demonstrated that microfibers could be dual functionalized with two proteins by simple simultaneous addition of proteins in excess concentration. As shown in Figure 6A and 6B, TCO microfibers were either incubated with **HaloTag-Tz** and **NanoLuc-Tz** simultaneously or sequentially in equimolar concentrations (1.25 μM) for 30 minutes. For sequential conjugation, **NanoLuc-Tz** was conjugated first, followed by three washes and then **HaloTag-Tz** was conjugated to the fibers. Subsequently, fibers were incubated with TAMRA-Cl (2 μM) and washed. The microfibers were then imaged using a fluorescence microscope, and then luminescence reading was measured following the addition of furimazine. The fibers that were functionalized through simultaneous conjugation of both proteins (Figure 6A) were both fluorescent (Figure 6C) and active in the luminescence assay (Figure 6D), indicating that the fibers were functionalized by both HaloTag and NanoLuc. TCO-decorated microfibers that were simultaneously conjugated with both

proteins were 80% as fluorescent as microfibers that were only conjugated to HaloTag and were considerably more fluorescent compared to the fibers where proteins were sequentially conjugated.

The luminescent activity of NanoLuc was also measured for these fibers, and compared to fibers that were conjugated to NanoLuc-only. The sequentially conjugated fibers retained 89% of the luminescent activity of the NanoLuc-only fibers. The low fluorescence and high luminescence from the sequentially conjugated fibers suggest that the initial conjugation of **NanoLuc-Tz** was efficient enough to saturate the majority of TCO-sites, leaving few sites for the conjugation of **HaloTag-Tz**. The simultaneously conjugated fibers retained 63% of the luminescent activity of the NanoLuc-only fibers. Thus, the method using simultaneous conjugation is amenable to the modification of the microfibers with multiple proteins that retain their individual functionality after attachment. A sequential conjugation experiment where **HaloTag-Tz** was conjugated first to the fibers, and then **NanoLuc-Tz** was conjugated, was also performed (Figure S9). In this case, the luminescence is within the background levels for non-photoactivated fibers (Fig 5B).

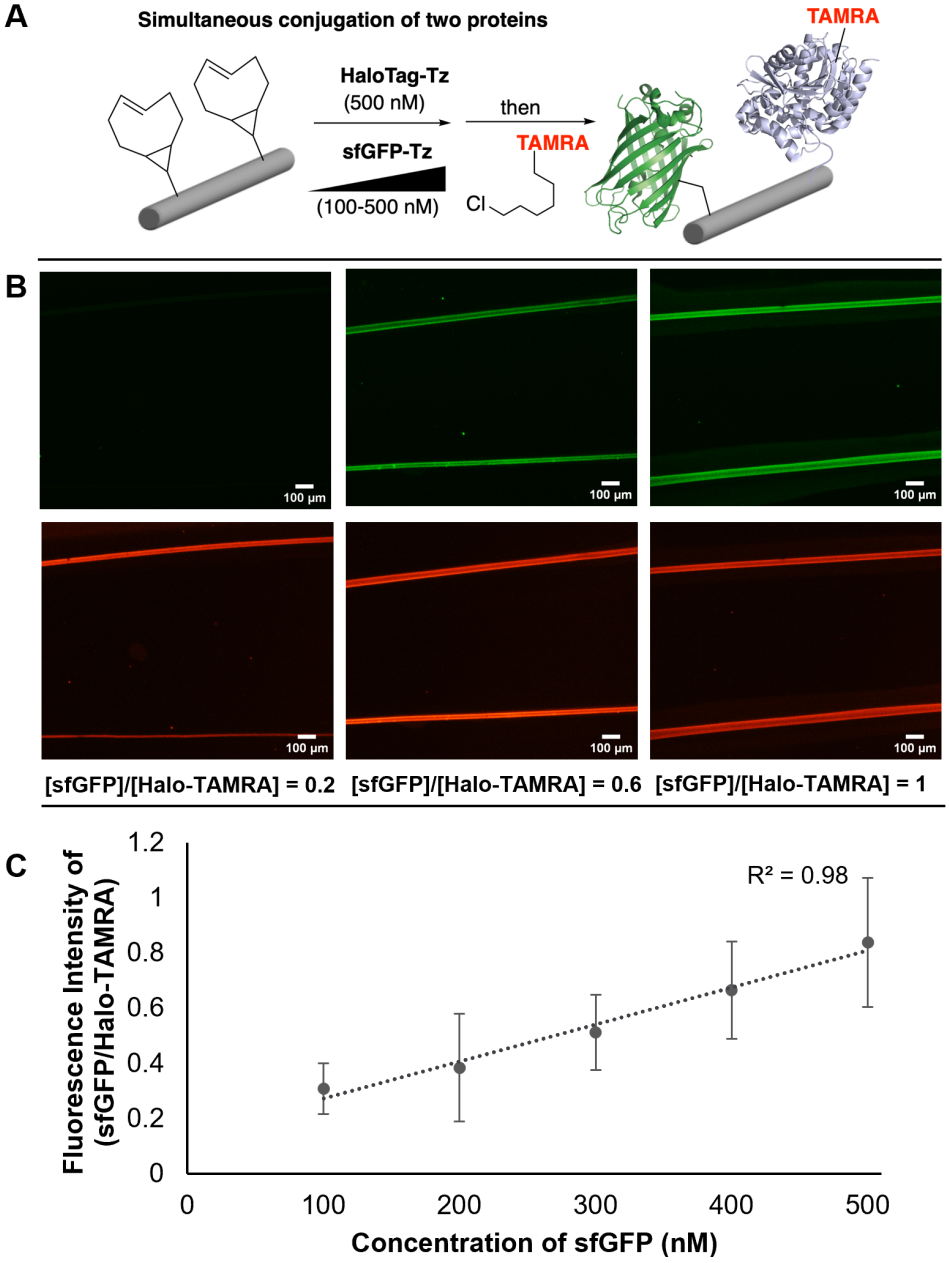

Figure 7. (A) The microfibers were incubated with a solution containing HaloTag-Tz (500 nM) and sfGFP-Tz that varied in concentration between 100-500 nM. TAMRA-Cl was added to obtain the fluorescent readout of HaloTag. (B) Fluorescence microscopy images were obtained for fibers simultaneously tagged with Halo-TAMRA (500 nM) and sfGFP (100 nM, 300 nM and 500 nM) (C) The ratio of fluorescence intensity of sfGFP:Halo-TAMRA was plotted against the concentration of sfGFP which showed a linear relationship (n=3).

Another advantage of late-stage functionalization of the microfibers is the control over the relative concentration of proteins presented on the surface of the fibers. To demonstrate this, we incubated the fibers with **HaloTag-Tz** and **sfGFP-Tz**[51] simultaneously, at a constant HaloTag-Tz

concentration of 500 nM and a **sfGFP-Tz** concentration varying from 100-500 nM (Figure 7A). TAMRA-Cl was added to the fibers to obtain the fluorescence output corresponding to the HaloTag concentration. sfGFP was modifed with PyTz using cysteine alkylation, with a cysteine genetically encoded at the C-terminal. sfGFP was singly modified with PyTz as verified my mass spectrometry (Figure S10).

The fluorescence densitometry from HaloTag-TAMRA and sfGFP were measured (Figure S11-S13) and the ratio of sfGFP:HaloTag-TAMRA was plotted. Figure 7C shows a linear increase of the fluorescence intensity ratio corresponding to the increase in the sfGFP concentration. The kinetics of reactions of **sfGFP-Tz** and **HaloTag-Tz** with sTCO was measured as described in the Supporting Information (Figure S14). Through a timecourse gain-of-fluorescence experiment, the second order rate constant for **sfGFP-Tz** was measured to be k_2 135,000 ± 5000 M^{-1} s^{-1}, and a competition experiment showed that the reactivity of **HaloTag-Tz** is indistinguishable within error. The number of TCO sites on the TCO microfibers was calculated to be ≤0.51 (± 0.12) pmol/cm of fiber, as described in the Supporting Information. Since the kinetics of the protein conjugation remains the same for both proteins, the proteins are competing for a limited number of TCO sites on the surface of the fibers leading to a linear increase in the amount of sfGFP-Tz being conjugated to the fibers in the concentration regime that was assayed.

Fibronectin-Functionalized Microfibers Promote Integrin-Mediated Cell Adhesion

We next sought to show that TCO-functionalized microfibers can be modified with biological cues that promote cell adhesion and cell growth. Previously, we showed that a TCO-tagged RGD peptide can be conjugated to microfibers after interfacial polymerization and photocatalytic DHTz activation.[33] We confirmed that RGD-modified microfibers promote the attachment and anisotropic spreading of fibroblasts. RGD is a common peptide motif found in a number of ECM proteins, including fibronectin, fibrinogen, osteopontin, and vitronectin.[57] While RGD peptides are commonly used in ECM-mimetic motifs,[43, 58] the short peptide cannot fully recapitulate the function of the complex protein. In fact, cell engagement with RGD-containing ECM proteins is highly selective, as individual proteins can distinguish between different types of integrins and differentially promote a range of cellular processes including migration, proliferation, survival, apoptosis, tumor invasion and metastasis.[59, 60] Therefore, it is beneficial to use full-length protein or protein domains to better replicate the environment provided by the ECM. Our protein of interest here is fibronectin type III domains 9-10 (FNIII 9-10). The RGD sequence present in domain 10 promotes cell adhesion and migration.[61] The Pro-His-Ser-Arg-Asn (PHSRN) sequence in domain 9 has a synergetic relationship with RGD in domain 10. Both are required for the binding of certain integrins, such as $\alpha_5\beta_1$, $\alpha_v\beta_3$, and $\alpha_{IIb}\beta_3$.[62-66]

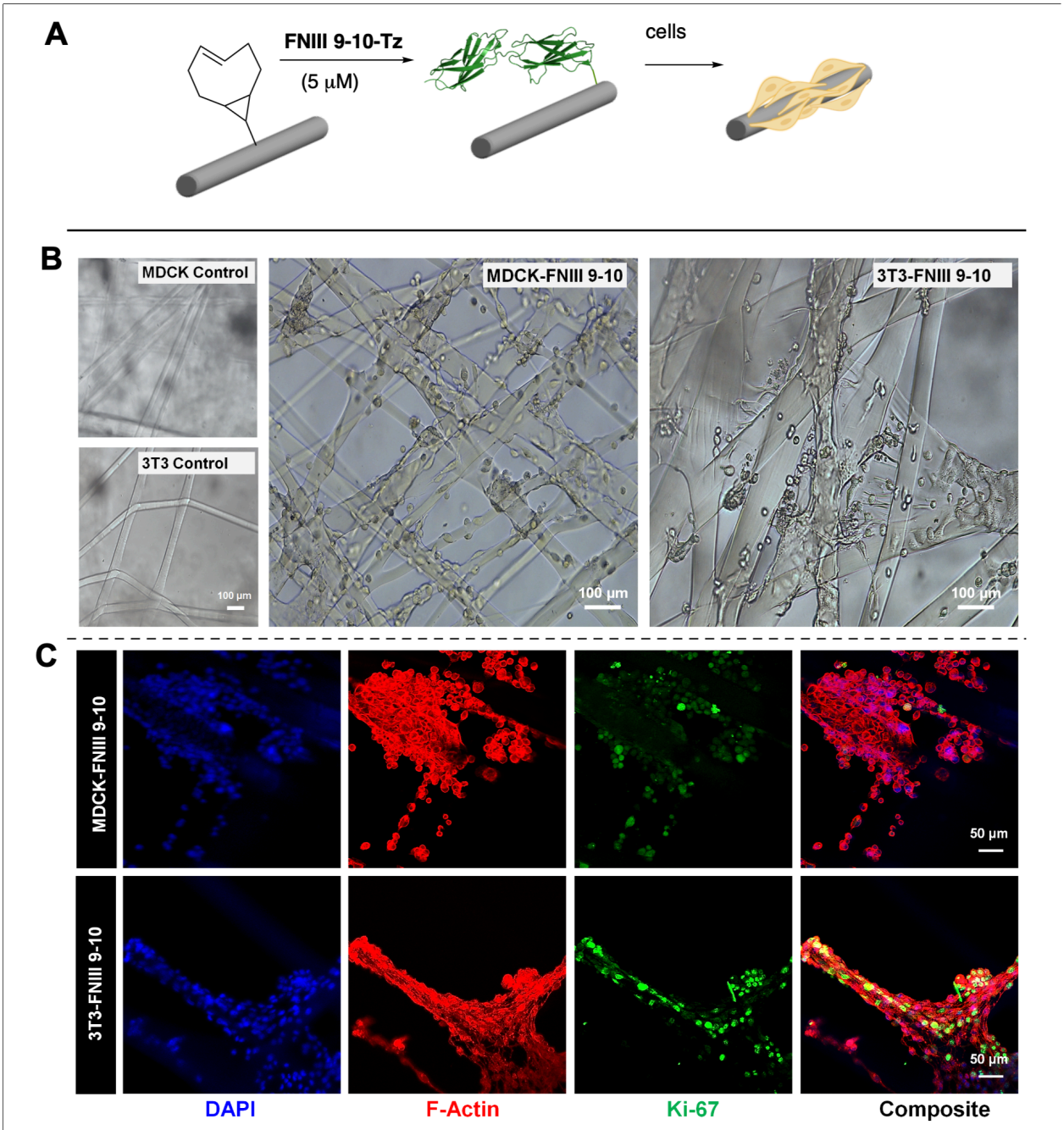

Figure 8: (A) Schematic showing TCO microfibers functionalized with FNIII 9-10. **(B)** Brightfield images of MDCK and NIH-3T3 fibroblasts on TCO microfibers functionalized with/without FNIII 9-10 at day 5 of culture. Cells attach, spread and appear to align with TCO microfibers functionalized with FNIII 9-10. **(C)** Proliferation of MDCK and NIH 3T3 fibroblast cells along the microfibers scaffold is assessed by the Ki67 proliferation (green) marker.

To this end, DHTz containing microfibers were photocatalytically activated to tetrazine, then incubated with bis-TCO (**3**) to produce TCO decorated microfibers, as described above. The resultant microfibers were then modified with 5 μM Tz-functionalized FNIII 9-10 (**FNIII 9-10-Tz**). MDCK (Madin-Darby canine kidney) cells and GFP-labeled NIH3T3 fibroblasts were seeded on glass bottom MatTek petri-dishes containing fiber scaffold laid over a central poly(2-hydroxyethyl methacrylate) coated non-adhesive area. Cell adhesion, viability, and proliferation were analyzed after 5 days of culture in growth media.

Microfibers that were derivatized by **FNIII 9-10-Tz** through late-stage functionalization promoted the attachment and spreading of both MDCK cells and NIH3T3 fibroblasts (**Figure 8 B**). Live/dead staining showed viability of 88 ± 5 % on day 1 to 90 ± 3% on day 5 of culture for MDCK cells (Figure S16). Both MDCK cells and fibroblasts appeared to grow beyond the confines of the fiber mesh, bridging adjacent fibers and fiber junctions (Figure S17, white arrowheads). The number of cells attached and spreading along fibers increased over time. Furthermore, cells attached to FNIII 9-10 decorated microfibers remained proliferative, as evidenced by positive staining for Ki-67, a cell proliferation marker (**Figure 8C**).

As a comparison, **FNIII 9-10-Tz** (5 μM) was directly incorporated into the microfibers during interfacial synthesis and fiber pulling. The resulting microfibers were non-adhesive to both MDCK and NIH3T3 cell lines after five days of culture (Figure S18). This loss of protein activity during interfacial polymerization mirrors what was observed with HaloTag incorporation, and likely indicates that the FNIII 9-10 protein was denatured during fiber pulling.

Conclusion

The site selective modification and purification of proteins by ABC-tagging allows for the modification of material surfaces with active proteins. Using hydrogel microfibers as a model system, we've shown that this methodology allows for the site-specific attachment and control over the relative concentration of the protein presented on the surface. The resulting microfibers have been shown to successfully conjugate to a range of proteins that retain their respective self-labeling, enzymatic, fluorescent and cell-adhesive properties. This methodology also supports the immobilization of multiple proteins on the microfiber surface, with the ability to control the relative concentrations of the different proteins presented on the surface by simply varying the stoichiometry of the proteins present in the solution during conjugation. This methodology enhances the toolkit of the methods for the surface modification of materials with functional proteins with the combined benefits of rapid tetrazine ligation and the site-selective Affinity Bioorthogonal Chemistry (ABC) protein tagging method.

Supporting Information

Procedures for the synthesis of compound **3,** plasmid cloning, protein purification, conjugation of 3-(2-pyridyl)-6-methyltetrazine to proteins, quantification of number of TCO sites on microfibers, kinetics of sfGFP-Tz and HaloTag-Tz with sTCO, mass spectra and NMR spectra

Acknowledgment. This work was supported by NSF through the University of Delaware Materials Research Science and Engineering Center, DMR-2011824, and by NIH (R01GM132460), (NIDCR R01 DE029655, NIDCD, R01DC014461), National Science Foundation (NSF, DMR 1809612). Instrumentation was supported by NIH awards P20GM104316, P20GM103446, S10OD025185, S10OD026951, S10OD016267, S10OD016361, and S10OD30321.

References

(1) Bhakta, S. A.; Evans, E.; Benavidez, T. E.; Garcia, C. D. Protein Adsorption onto Nanomaterials for the Development of Biosensors and Analytical Devices: A review. *Anal. Chim. Acta* **2015**, *872*, 7-25. DOI: https://doi.org/10.1016/j.aca.2014.10.031.
(2) Rusmini, F.; Zhong, Z.; Feijen, J. Protein Immobilization Strategies for Protein Biochips. *Biomacromolecules* **2007**, *8*, 1775-1789. DOI: 10.1021/bm061197b.
(3) Lee, J. P.; Kassianidou, E.; MacDonald, J. I.; Francis, M. B.; Kumar, S. N-Terminal Specific Conjugation of Extracellular Matrix Proteins to 2-Ppridinecarboxaldehyde Functionalized Polyacrylamide Hydrogels. *Biomaterials* **2016**, *102*, 268-276. DOI: https://doi.org/10.1016/j.biomaterials.2016.06.022.
(4) Wylie, R. G.; Ahsan, S.; Aizawa, Y.; Maxwell, K. L.; Morshead, C. M.; Shoichet, M. S. Spatially Controlled Simultaneous Patterning of Multiple Growth Factors in Three-dimensional Hydrogels. *Nat. Mater.* **2011**,*10*, 799-806. DOI: 10.1038/nmat3101.
(5) Stie, M. B.; Kalouta, K.; Vetri, V.; Foderà, V. Protein Materials as Sustainable Non- and Minimally Invasive Strategies for Biomedical Applications. *J. Control. Release* **2022**, *344*, 12-25. DOI: https://doi.org/10.1016/j.jconrel.2022.02.016.
(6) Wang, Y.; Katyal, P.; Montclare, J. K. Protein-Engineered Functional Materials. *Adv. Healthc. Mater.* **2019**, *8*, 1801374. DOI: https://doi.org/10.1002/adhm.201801374.
(7) Cha, T.; Guo, A.; Zhu, X.-Y. Enzymatic Activity on a Chip: The Critical Role of Protein Orientation. *Proteomics* **2005**, *5*, 416-419. DOI: https://doi.org/10.1002/pmic.200400948.
(8) Wu, J. C. Y.; Hutchings, C. H.; Lindsay, M. J.; Werner, C. J.; Bundy, B. C. Enhanced Enzyme Stability Through Site-Directed Covalent Immobilization. *J. Biotechnol.* **2015**, *193*, 83-90. DOI: https://doi.org/10.1016/j.jbiotec.2014.10.039.
(9) Santos, M. P. F.; Brito, M. J. P.; Junior, E. C. S.; Bonomo, R. C. F.; Veloso, C. M. Pepsin Immobilization on Biochar by Adsorption and Covalent Binding, and its Application for Hydrolysis of Bovine Casein. *J. Chem. Technol. Biotechnol.* **2019**, *94*, 1982-1990. DOI: https://doi.org/10.1002/jctb.5981.
(10) Gilbert, S. F. *Developmental Biology, 6th edition*; Sinauer Associates, 2000.
(11) Shadish, J. A.; DeForest, C. A. Site-Selective Protein Modification: From Functionalized Proteins to Functional Biomaterials. *Matter* **2020**, *2*, 50-77. DOI: https://doi.org/10.1016/j.matt.2019.11.011.
(12) Raliski, B. K.; Howard, C. A.; Young, D. D. Site-Specific Protein Immobilization Using Unnatural Amino Acids. *Bioconj. Chem.* **2014**, *25*, 1916-1920. DOI: 10.1021/bc500443h.
(13) Spicer, C. D.; Pashuck, E. T.; Stevens, M. M. Achieving Controlled Biomolecule–Biomaterial Conjugation. *Chem. Rev.* **2018**, *118*, 7702-7743. DOI: 10.1021/acs.chemrev.8b00253.
(14) Chalker, J. M.; Bernardes, G. J. L.; Lin, Y. A.; Davis, B. G. Chemical Modification of Proteins at Cysteine: Opportunities in Chemistry and Biology. *Chem. Asian J.* **2009**, *4*, 630-640. DOI: https://doi.org/10.1002/asia.200800427.
(15) Chen, Y.-X.; Triola, G.; Waldmann, H. Bioorthogonal Chemistry for Site-Specific Labeling and Surface Immobilization of Proteins. *Acc. Chem. Res.* **2011**, *44*, 762-773. DOI: 10.1021/ar200046h.
(16) Kölmel, D. K.; Kool, E. T. Oximes and Hydrazones in Bioconjugation: Mechanism and Catalysis. *Chem. Rev.* **2017**, *117*, 10358-10376. DOI: 10.1021/acs.chemrev.7b00090.
(17) Lempens, E. H. M.; Helms, B. A.; Merkx, M.; Meijer, E. W. Efficient and Chemoselective Surface Immobilization of Proteins by Using Aniline-Catalyzed Oxime Chemistry. *ChemBioChem* **2009**, *10*, 658-662. DOI: https://doi.org/10.1002/cbic.200900028.

(18) Bednarek, C.; Wehl, I.; Jung, N.; Schepers, U.; Bräse, S. The Staudinger Ligation. *Chem. Rev.* **2020**, *120*, 4301-4354. DOI: 10.1021/acs.chemrev.9b00665.
(19) Bian, S.; Schesing, K. B.; Braunschweig, A. B. Matrix-assisted Polymer Pen Lithography Induced Staudinger Ligation. *Chem. Commun.* **2012**, *48*, 4995-4997, 10.1039/C2CC31615C. DOI: 10.1039/C2CC31615C.
(20) Vutti, S.; Buch-Månson, N.; Schoffelen, S.; Bovet, N.; Martinez, K. L.; Meldal, M. Covalent and Stable CuAAC Modification of Silicon Surfaces for Control of Cell Adhesion. *ChemBioChem* **2015**, *16*, 782-791. DOI: https://doi.org/10.1002/cbic.201402629.
(21) Devaraj, N. K.; Collman, J. P. Copper Catalyzed Azide-Alkyne Cycloadditions on Solid Surfaces: Applications and Future Directions. *QSAR & Combinatorial Science* **2007**, *26*, 1253-1260. DOI: https://doi.org/10.1002/qsar.200740121.
(22) Nandivada, H.; Lahann, J. Copper-Catalyzed 'Click' Chemistry for Surface Engineering. In *Click Chemistry for Biotechnology and Materials Science*, 2009; pp 291-307.
(23) Hayat, A.; Sassolas, A.; Rhouati, A.; Marty, J.-L. Immobilization of Enzymes on Ethynyl-Modified Electrodes via Click Chemistry. In *Immobilization of Enzymes and Cells: Third Edition*, Guisan, J. M. Ed.; Humana Press, 2013; pp 209-216.
(24) Vrettou, F.; Petrou, P.; Kakabakos, S.; Argitis, P.; Gajos, K.; Budkowski, A.; Chatzichristidi, M. Surface Modification for Site-directed Covalent Attachment of Molecules via Strain-promoted Azide-alkyne Click-chemistry Reaction and Photolithography. *Surfaces and Interfaces* **2023**, *36*, 102500. DOI: https://doi.org/10.1016/j.surfin.2022.102500.
(25) Wendeln, C.; Singh, I.; Rinnen, S.; Schulz, C.; Arlinghaus, H. F.; Burley, G. A.; Ravoo, B. J. Orthogonal, Metal-Free Surface Modification by Strain-promoted Azide–alkyne and Nitrile oxide–alkene/alkyne Cycloadditions. *Chem. Sci.* **2012**, *3*, 2479-2484. DOI: 10.1039/C2SC20555F.
(26) Chaparro Sosa, A. F.; Bednar, R. M.; Mehl, R. A.; Schwartz, D. K.; Kaar, J. L. Faster Surface Ligation Reactions Improve Immobilized Enzyme Structure and Activity. *J. Am. Chem. Soc.* **2021**, *143*, 7154-7163. DOI: 10.1021/jacs.1c02375.
(27) Blackman, M. L.; Royzen, M.; Fox, J. M. Tetrazine Ligation: Fast Bioconjugation Based on Inverse-Electron-Demand Diels–Alder Reactivity. *J. Am. Chem. Soc.* **2008**, *130*, 13518-13519. DOI: 10.1021/ja8053805.
(28) Darko, A.; Wallace, S.; Dmitrenko, O.; Machovina, M. M.; Mehl, R. A.; Chin, J. W.; Fox, J. M. Conformationally Strained *trans*-Cyclooctene with Improved Stability and Excellent Reactivity in Tetrazine Ligation. *Chem. Sci.* **2014**, *5*, 3770-3776. DOI: 10.1039/C4SC01348D.
(29) Oliveira, B. L.; Guo, Z.; Bernardes, G. J. L. Inverse Electron Demand Diels–Alder reactions in Chemical Biology. *Chem. Soc. Rev.* **2017**, *46*, 4895-4950. DOI: 10.1039/C7CS00184C.
(30) Arkenberg, M. R.; Kim, M. H.; Lin, C.-C. Click Hydrogels for Biomedical Applications. In *Multicomponent Hydrogels: Smart Materials for Biomedical Applications*, Dodda, J. M., Deshmukh, K., Bezuidenhout, D. Eds.; The Royal Society of Chemistry, 2023; p 0. DOI: 10.1039/BK9781837670055-00155.
(31) Zhang, C.-J.; Tan, C. Y. J.; Ge, J.; Na, Z.; Chen, G. Y. J.; Uttamchandani, M.; Sun, H.; Yao, S. Q. Preparation of Small-Molecule Microarrays by trans-Cyclooctene Tetrazine Ligation and Their Application in the High-Throughput Screening of Protein–Protein Interaction Inhibitors of Bromodomains. *Angew. Chem. Int. Edit.* **2013**, *52*, 14060-14064. DOI: https://doi.org/10.1002/anie.201307803.
(32) Wang, P.; Na, Z.; Fu, J.; Tan, C. Y. J.; Zhang, H.; Yao, S. Q.; Sun, H. Microarray Immobilization of Biomolecules using a Fast *trans*-Cyclooctene (TCO)–Tetrazine Reaction. *Chem. Commun.* **2014**, *50*, 11818-11821. DOI: 10.1039/C4CC03838J.
(33) Zhang, H.; Trout, W. S.; Liu, S.; Andrade, G. A.; Hudson, D. A.; Scinto, S. L.; Dicker, K. T.; Li, Y.; Lazouski, N.; Rosenthal, J.; Thorpe, C.; Jia, X.; Fox, J. M. Rapid Bioorthogonal Chemistry

Turn-on through Enzymatic or Long Wavelength Photocatalytic Activation of Tetrazine Ligation. *J. Am. Chem. Soc.* **2016**, *138* , 5978-5983. DOI: 10.1021/jacs.6b02168.
(34) Bednar, R. M.; Golbek, T. W.; Kean, K. M.; Brown, W. J.; Jana, S.; Baio, J. E.; Karplus, P. A.; Mehl, R. A. Immobilization of Proteins with Controlled Load and Orientation. *ACS Appl. Mater. Interfaces* **2019**, *11*, 36391-36398. DOI: 10.1021/acsami.9b12746.
(35) Hast, K.; Stone, M. R.; Jia, Z.; Baci, M.; Aggarwal, T.; Izgu, E. C. Bioorthogonal Functionalization of Material Surfaces with Bioactive Molecules. *ACS Appl. Mater. Interfaces* **2023**, *15*, 4996-5009. DOI: 10.1021/acsami.2c20942.
(36) Jivan, F.; Alge, D. L. Bio-Orthogonal, Site-Selective Conjugation of Recombinant Proteins to Microporous Annealed Particle Hydrogels for Tissue Engineering. *Adv. Therap.* **2020**, *3*, 1900148. DOI: https://doi.org/10.1002/adtp.201900148.
(37) Putti, M.; de Jong, S. M. J.; Stassen, O. M. J. A.; Sahlgren, C. M.; Dankers, P. Y. W. A Supramolecular Platform for the Introduction of Fc-Fusion Bioactive Proteins on Biomaterial Surfaces. *ACS Appl. Polym. Mater.* **2019**, *1*, 2044-2054. DOI: 10.1021/acsapm.9b00334.
(38) Goor, O. J. G. M.; Keizer, H. M.; Bruinen, A. L.; Schmitz, M. G. J.; Versteegen, R. M.; Janssen, H. M.; Heeren, R. M. A.; Dankers, P. Y. W. Efficient Functionalization of Additives at Supramolecular Material Surfaces. *Adv. Mater.* **2017**, *29*, 1604652. DOI: https://doi.org/10.1002/adma.201604652.
(39) Özbek, N.; Sahkulubey Kahveci, E. L.; Kahveci, M. U. Light-Induced Inverse Electron Demand Diels–Alder Reaction as an Approach for Grafting Macromolecules to Glass Surfaces. *ACS Appl. Polym. Mater.* **2021**, *3*, 3721-3732. DOI: 10.1021/acsapm.1c00031.
(40) Jung, S.; Abel, J. H.; Starger, J. L.; Yi, H. Porosity-Tuned Chitosan–Polyacrylamide Hydrogel Microspheres for Improved Protein Conjugation. *Biomacromolecules* **2016**, *17*, 2427-2436. DOI: 10.1021/acs.biomac.6b00582.
(41) García-Maceira, T.; García-Maceira, F. I.; González-Reyes, J. A.; Torres-Sánchez, L. A.; Aragón-Gómez, A. B.; García-Rubiño, M. E.; Paz-Rojas, E. Covalent Immobilization of Antibodies through Tetrazine-TCO Reaction to Improve Sensitivity of ELISA Technique. In *Biosensors*, 2021; Vol. 11.
(42) Nikolova, M. P.; Chavali, M. S. Recent Advances in Biomaterials for 3D scaffolds: A Review. *Bioact. Mater.* **2019**, *4*, 271-292. DOI: 10.1016/j.bioactmat.2019.10.005 From NLM.
(43) Liu, S.; Zhang, H.; Remy, R. A.; Deng, F.; Mackay, M. E.; Fox, J. M.; Jia, X. Meter-Long Multiblock Copolymer Microfibers Via Interfacial Bioorthogonal Polymerization. *Adv. Mater.* **2015**, *27*, 2783-2790. DOI: 10.1002/adma.201500360.
(44) Liu, S.; Moore, A. C.; Zerdoum, A. B.; Zhang, H.; Scinto, S. L.; Zhang, H.; Gong, L.; Burris, D. L.; Rajasekaran, A. K.; Fox, J. M.; Jia, X. Cellular Interactions with Hydrogel Microfibers Synthesized via Interfacial Tetrazine Ligation. *Biomaterials* **2018**, *180*, 24-35. DOI: 10.1016/j.biomaterials.2018.06.042.
(45) George, O. J.; Song, J.; Benson, J. M.; Fang, Y.; Zhang, H.; Burris, D. L.; Fox, J. M.; Jia, X. Tunable Synthesis of Hydrogel Microfibers via Interfacial Tetrazine Ligation. *Biomacromolecules* **2022**, *23*, 3017-3030. DOI: 10.1021/acs.biomac.2c00504.
(46) Lam, A. J.; St-Pierre, F.; Gong, Y.; Marshall, J. D.; Cranfill, P. J.; Baird, M. A.; McKeown, M. R.; Wiedenmann, J.; Davidson, M. W.; Schnitzer, M. J.; Tsien, R. Y.; Lin, M. Z. Improving FRET Dynamic Range with Bright Green and Red Fluorescent Proteins. *Nat. Methods.* **2012**, *9*, 1005-1012. DOI: 10.1038/nmeth.2171.
(47) Pédelacq, J.-D.; Cabantous, S.; Tran, T.; Terwilliger, T. C.; Waldo, G. S. Engineering and Characterization of a Superfolder Green Fluorescent Protein. *Nat. Biotechnol.* **2006**, *24*, 79-88. DOI: 10.1038/nbt1172.
(48) Seitchik, J. L.; Peeler, J. C.; Taylor, M. T.; Blackman, M. L.; Rhoads, T. W.; Cooley, R. B.; Refakis, C.; Fox, J. M.; Mehl, R. A. Genetically Encoded Tetrazine Amino Acid Directs Rapid

Site-Specific in Vivo Bioorthogonal Ligation with *trans*-Cyclooctenes. *J. Am. Chem. Soc.* **2012**, *134*, 2898-2901. DOI: 10.1021/ja2109745.
(49) Blizzard, R. J.; Backus, D. R.; Brown, W.; Bazewicz, C. G.; Li, Y.; Mehl, R. A. Ideal Bioorthogonal Reactions Using A Site-Specifically Encoded Tetrazine Amino Acid. *J. Am. Chem. Soc.* **2015**, *137*, 10044-10047. DOI: 10.1021/jacs.5b03275.
(50) Mayer, S. V.; Murnauer, A.; von Wrisberg, M.-K.; Jokisch, M.-L.; Lang, K. Photo-induced and Rapid Labeling of Tetrazine-Bearing Proteins via Cyclopropenone-Caged Bicyclononynes. *Angew. Chem. Int. Ed.* **2019**, *58*, 15876-15882. DOI: https://doi.org/10.1002/anie.201908209.
(51) Scinto, S. L.; Reagle, T. R.; Fox, J. M. Affinity Bioorthogonal Chemistry (ABC) Tags for Site-Selective Conjugation, On-Resin Protein-Protein Coupling, and Purification of Protein Conjugates. *Angew. Chem. Int. Ed.* **2022**, *61*, e202207661. DOI: 10.1002/anie.202207661.
(52) Shadish, J. A.; Benuska, G. M.; DeForest, C. A. Bioactive site-specifically modified proteins for 4D patterning of gel biomaterials. *Nat. Mater.* **2019**, *18*, 1005-1014. DOI: 10.1038/s41563-019-0367-7.
(53) Gawade, P. M.; Shadish, J. A.; Badeau, B. A.; DeForest, C. A. Logic-Based Delivery of Site-Specifically Modified Proteins from Environmentally Responsive Hydrogel Biomaterials. *Adv. Mater.* **2019**, *31*, 1902462. DOI: https://doi.org/10.1002/adma.201902462.
(54) Glasgow, J. E.; Salit, M. L.; Cochran, J. R. In Vivo Site-Specific Protein Tagging with Diverse Amines Using an Engineered Sortase Variant. *J. Am. Chem. Soc.* **2016**, *138*, 7496-7499. DOI: 10.1021/jacs.6b03836.
(55) Los, G. V.; Encell, L. P.; McDougall, M. G.; Hartzell, D. D.; Karassina, N.; Zimprich, C.; Wood, M. G.; Learish, R.; Ohana, R. F.; Urh, M.; Simpson, D.; Mendez, J.; Zimmerman, K.; Otto, P.;Vidugiris, G.; Zhu, J.; Darzins, A.; Klaubert, D. H.; Bulleit, R. F.; Wood, K. V. HaloTag: A Novel Protein Labeling Technology for Cell Imaging and Protein Analysis. *ACS Chem. Biol.* **2008**, *3*, 373-382. DOI: 10.1021/cb800025k.
(56) Hall, M. P.; Unch, J.; Binkowski, B. F.; Valley, M. P.; Butler, B. L.; Wood, M. G.; Otto, P.; Zimmerman, K.; Vidugiris, G.; Machleidt, T.; Robers, M. B.; Benink, H. A.; Eggers, C. T.; Slater, M. R.; Meisenheimer, P. L.; Klaubert, D. H.; Fan, F.; Encell, L. P.; Wood, K. V. Engineered Luciferase Reporter from a Deep Sea Shrimp Utilizing a Novel Imidazopyrazinone Substrate. *ACS Chem. Biol.* **2012**, *7*, 1848-1857. DOI: 10.1021/cb3002478.
(57) Plow, E. F.; Haas, T. A.; Zhang, L.; Loftus, J.; Smith, J. W. Ligand Binding to Integrins. *J. Biol. Chem.* **2000**, *275*, 21785-21788. DOI: 10.1074/jbc.R000003200.
(58) Pol, M.; Gao, H.; Zhang, H.; George, O. J.; Fox, J. M.; Jia, X. Dynamic Modulation of Matrix Adhesiveness Induces Epithelial-to-mesenchymal Transition in Prostate Cancer Cells in 3D. *Biomaterials* **2023**, *299*, 122180. DOI: https://doi.org/10.1016/j.biomaterials.2023.122180.
(59) Kapp, T. G.; Rechenmacher, F.; Neubauer, S.; Maltsev, O. V.; Cavalcanti-Adam, E. A.; Zarka, R.; Reuning, U.; Notni, J.; Wester, H.-J.; Mas-Moruno, C.; Spatz, J.; Geiger, B.; Kessler, H. A Comprehensive Evaluation of the Activity and Selectivity Profile of Ligands for RGD-binding Integrins. *Sci. Rep.* **2017**, *7*, 39805. DOI: 10.1038/srep39805.
(60) Mould, A. P.; Humphries, M. J. Adhesion Articulated. *Nature* **2004**, *432*, 27-28. DOI: 10.1038/432027a.
(61) Ruoslahti, E. RGD and Other Recognition Sequences For Integrins. *Annu. Rev. Cell Dev. Biol.* **1996**, *12*, 697-715. DOI: 10.1146/annurev.cellbio.12.1.697.
(62) Li, S.; Nih, L. R.; Bachman, H.; Fei, P.; Li, Y.; Nam, E.; Dimatteo, R.; Carmichael, S. T.; Barker, T. H.; Segura, T. Hydrogels with Precisely Controlled Integrin Activation Dictate Vascular Patterning and Permeability. *Nat. Mater.* **2017**, *16*, 953-961. DOI: 10.1038/nmat4954.
(63) Grant, R. P.; Spitzfaden, C.; Altroff, H.; Campbell, I. D.; Mardon, H. J. Structural Requirements for Biological Activity of the Ninth and Tenth FIII Domains of Human Fibronectin*. *J. Biol. Chem.* **1997**, *272*, 6159-6166. DOI: https://doi.org/10.1074/jbc.272.10.6159.

(64) Aota, S.; Nomizu, M.; Yamada, K. M. The Short Amino Acid Sequence Pro-His-Ser-Arg-Asn in Human Fibronectin Enhances Cell-adhesive Function. *J. Biol. Chem.* **1994**, *269*, 24756-24761. DOI: https://doi.org/10.1016/S0021-9258(17)31456-4.
(65) Bowditch, R. D.; Hariharan, M.; Tominna, E. F.; Smith, J. W.; Yamada, K. M.; Getzoff, E. D.; Ginsberg, M. H. Identification of a Novel Integrin Binding Site in Fibronectin. Differential Utilization by beta 3 Integrins. *J. Biol. Chem.* **1994**, *269*, 10856-10863. DOI: https://doi.org/10.1016/S0021-9258(17)34137-6.
(66) Akiyama, S. K.; Aota, S.-I.; Yamada, K. M. Function and Receptor Specificity of a Minimal 20 Kilodalton Cell Adhesive Fragment of Fibronectin. *Cell Adhes. Commun.* **1995**, *3*, 13-25. DOI: 10.3109/15419069509081275.

TOC graphic

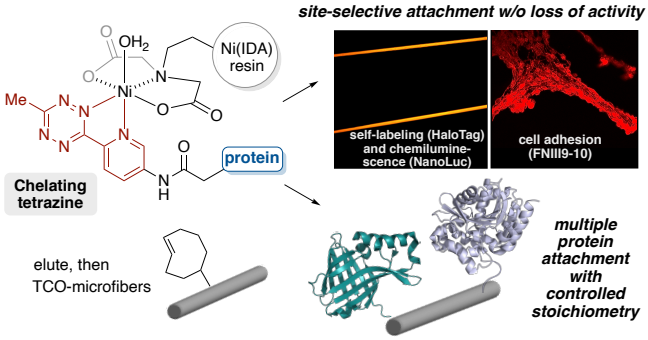
site-selective attachment w/o loss of activity
Ni(IDA) resin
protein
Chelating tetrazine
self-labeling (HaloTag) and chemilumine-scence (NanoLuc)
cell adhesion (FNIII9-10)
elute, then TCO-microfibers
multiple protein attachment with controlled stoichiometry